

# MODELING OF NO AND OH INFRARED RADIATION ON A CONVERGENT-DIVERGENT NOZZLE

Hyun Jae Nam, Jae Won Kim and Oh Joon Kwon\*  
 Korea Advanced Institute of Science and Technology  
 namjae@kaist.ac.kr; guonetoo@kaist.ac.kr; ojkwon@kaist.ac.kr

**Keywords:** Radiation modeling, Intensity simulation, Nonequilibrium flow

## Abstract

*In the present study, modeling of infrared radiation for NO and OH diatomic molecules involved with the absorption by room air was carried out for the use in nonequilibrium radiation simulations. The line positions for NO and OH were determined by diagonalizing the Hamiltonian matrices of each molecule. The Einstein coefficients were utilized to calculate the temperature-related line intensities. It was shown that the computed spectral intensity is in good agreement with the measured spectrum. Assessment of the effect of room air absorption on radiation intensity showed that the radiation spectrum is attenuated by the room air absorption in the range of 2.4-3.2  $\mu\text{m}$  and 4.9-5.5  $\mu\text{m}$ . The radiation intensity of the one-dimensional steady flow through a convergent-divergent nozzle under thermal nonequilibrium condition was also analyzed. Highly intense emission in the range of 5.3-5.5  $\mu\text{m}$ , which is similar to the results at the same translational and rotational temperatures of 200 K, was observed.*

## 1 Introduction

Up until recently, much effort has been made to analyze the nonequilibrium phenomena behind the bow shock wave forming in front of the nose of hypersonic re-entry vehicles as they cross the atmosphere. It was known that radiation peak exists in the nonequilibrium region behind the shock wave, and the radiative heat transfer in the ultraviolet and visible wavelength range is the main heat source. In contrast, for the ground-based infrared signature detection for

converging-diverging nozzles, the heat transfer and the infrared spectral emission and absorption of air are also important, even though they are relatively small compared to those observed during re-entry. To determine the temperature and the concentration for optical diagnostics, accurate radiation models are required in both equilibrium and nonequilibrium. Especially, nitric oxide (NO) plays an important role in the chemistry of the nozzle flow, since hydroxyl radical (OH) is important in the combustion process.

The spectrum of such gaseous medium was obtained mostly by relying on experimental tests [1-2]. In addition, some efforts have been made for estimating the radiation intensity in the visible and ultraviolet wavelength range [3-6]. However, relatively less effort has been made in the infrared range. Laux et al. [7] performed accurate measurements and numerical predictions for air plasma in the infrared. Packan et al. [8] analyzed the infrared radiation of air plasma in a local thermodynamic equilibrium through measurements and numerical simulations.

It is known that in the divergent section, the nozzle flow shows freezing of the atomic recombination process, which represents thermally nonequilibrium phenomenon [9]. However, the flow-field calculation in the convergent-divergent nozzle is frequently performed under equilibrium conditions, which results in the temperature difference compared to those of nonequilibrium conditions.

In the present study, a numerical methodology has been developed such that the infrared transition of both NO and OH diatomic molecules can be estimated. Then assessment of the effect of room air absorption was performed

by comparing the results without the absorption. The radiation intensity of the flow through a convergent-divergent nozzle under a thermal nonequilibrium condition is also presented.

## 2 Infrared Radiation Model

### 2.1 Modeling of *NO* and *OH* Molecules with Water Absorption

To estimate the spectral line position and the intensity in the infrared region by the transition of the two diatomic molecules, an accurate line-by-line radiation model is required. For this purpose, an existing radiation package, the Structured Package for Radiation Analysis 2007 code (*SPRADIAN07*) [10], was adopted for calculating the emission and the absorption of the diatomic molecules. The package solves the radiative transfer equation:

$$\frac{dI_\lambda}{ds} = \varepsilon_\lambda - k_\lambda I_\lambda \quad (1)$$

where  $I_\lambda$  is the spectral intensity, and  $s$  is the optical path along the line of sight.  $\varepsilon_\lambda$  and  $k_\lambda$  are the emission and absorption coefficients, and are also computed by using the line-by-line technique. However, the existing code lacks the capability of determining the rotational energy in the infrared range. To overcome this limitation, a new module was implemented such that the Hamiltonian matrices for *NO* and *OH* molecules to determine the rotational energy and the line position can be diagonalized. The detailed information about the Hamiltonian matrix of *NO* and *OH* are given in the work by Amiot [11] and Stark, Brault and Abrams [12] with a correction to the work by Levin, Laux and Kruger [5]. According to the Hamiltonian matrix, the vibrational quantum numbers of *NO* and *OH* are up to 22 and 2, and the rotational quantum numbers are up to 59.5 and 30.5, respectively. The module also enables to compute the six main branches and the six satellite branches of the transition, vibrational, and rotational partition functions [13]. The Einstein coefficients of *NO* obtained from the

work by Langhoff and Bauschlicher [14] was utilized to determine the temperature-related line intensities. In the case of *OH* molecule, it is known that the transition probabilities in the IR wavelength range exhibit a unique distribution because of the very strong dependence on the centrifugal distortion of the vibrational potentials. Thus, in the present study, the Einstein coefficients of *OH* molecules were obtained from the work by Holtzclaw, Person and Green [15]. As a result of the infrared radiation modeling, the module enables to calculate the fundamental ( $\Delta v = 1$ ) and first overtone ( $\Delta v = 2$ ) rovibrational bands of *NO* and the fundamental rovibrational bands of *OH*.

To estimate the effect of the absorption by air consisted of  $H_2O$  and  $CO_2$ , the characteristics of both  $H_2O$  and  $CO_2$  should be known. The absorption calculations for  $H_2O$  and  $CO_2$  can be obtained by utilizing the high-resolution database, *HITEMP* [16], which is an extended version of *HITRAN* [17]. Due to the limitation of the calculating partition function, this database is applicable up to the temperature of 3000 K. The attenuation of the emission spectrum with water absorption was taken into account by adopting Beer's law. For the comparison, the spectral transmittances of both water vapor and carbon dioxide were calculated under the conditions obtained from the work of Packman et al. [8]. In the calculation, the following parameters were used: temperature of 298 K, optical length of six meters,  $H_2O$  mole fraction of 0.013, and  $CO_2$  mole fraction of 0.033.

In Figs. 1 and 2, the calculated transmittance of water vapor and carbon dioxide over the spectral ranges between  $1.5 \mu m$  and  $5.5 \mu m$  are presented, respectively. It was observed in Fig. 1 that the strong absorption occurs at  $2.7 \mu m$  and near  $5.5 \mu m$ . The spectral transmittance of  $CO_2$  in Fig. 2 reduces to about 0.6 at  $2.7 \mu m$ , and is very close to 0 at  $4.3 \mu m$ .

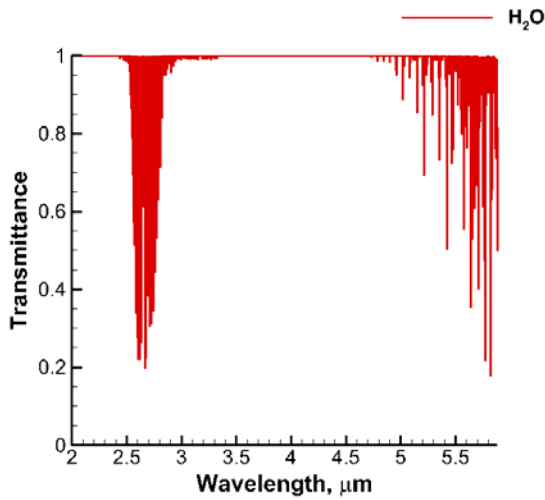


Fig. 1. Spectral Transmittance of  $H_2O$  with Path Length of Six Meter.

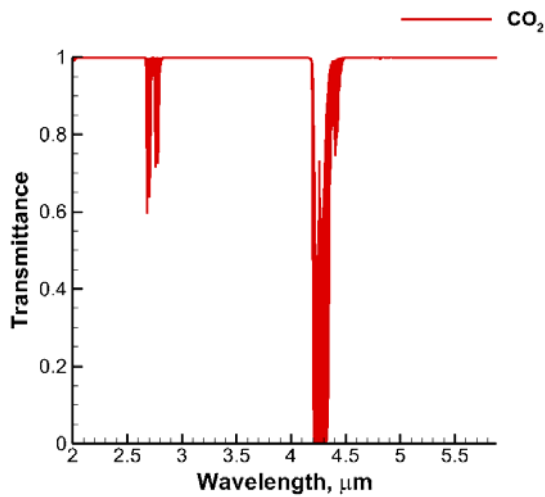


Fig. 2. Spectral Transmittance of  $CO_2$  with Path Length of Six Meter.

## 2.2 Thermal Nonequilibrium in Convergent-Divergent Nozzle

It is well known that gas flows expanding through a nozzle exhibit thermal nonequilibrium phenomena [9]. To consider the thermal nonequilibrium properly, estimation of the properties of the expanding flow is necessary. This can be done by performing space-marching calculations of the one-dimensional steady flows through the convergent-divergent nozzle in the dissociated and ionized regimes. In the present study, an equilibrium condition was assumed at the entrance of the nozzle, and at the downstream from the nozzle throat a multi-temperature nonequilibrium was assumed. To

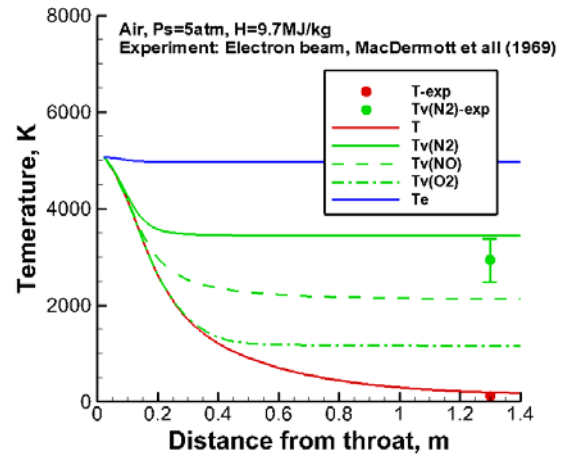


Fig. 3. Comparison between Calculated and Measured Temperatures along Nozzle in Air under Two-temperature Model.

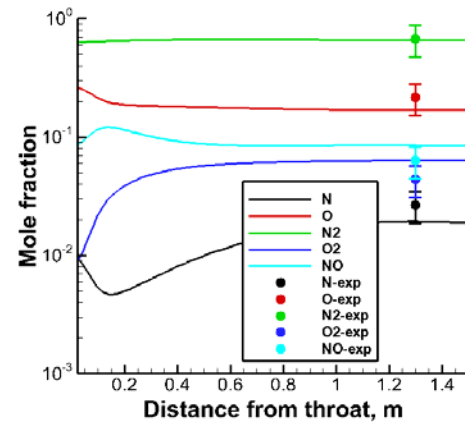


Fig. 4. Comparison between the Calculated and Measured Mole Fractions along Nozzle in Air.

determine the rate coefficients, various temperatures were used. In particular, the vibrational and electron-electronic temperatures were calculated by integrating the governing rate equations by accounting for the vibration-to-translation, vibration-to-vibration, vibration-to-electron thermal, and vibration-to-electronic energy transfer mechanisms, and the radiative cooling. It was assumed that the heavy-particle translational temperature is equal to the rotational temperature, and the vibrational temperatures of  $NO$ ,  $N_2$  and  $O_2$  are different from each other. The chemical reactions were computed by using a two-temperature model proposed by Park [18]. From the calculation of

the nozzle flow, various temperatures and mole fractions can be determined.

Comparison between the calculated and measured temperatures is presented along the nozzle in the air in Fig. 3. It is shown that the results of the present calculation match well with the experimental measurement [19]. The figure also shows the freezing of the atomic recombination process in the vibrational temperature. It was observed that the vibrational temperature and the translational temperature were 2135 and 200 K at the distance of 1.2 m from the throat, respectively. In a same manner, the value of the mole fraction of NO was 0.0854 as shown in Fig. 4.

### 3 Results and discussion

#### 3.1 Infrared Spectrum of NO and OH Molecules with Water Absorption

In the present study, the computed wavelength range was set between 2.5  $\mu\text{m}$  and 5.5  $\mu\text{m}$  to capture the rovibrational bands of both NO and OH molecules. The spectrum over the given range was calculated by using the present radiation nonequilibrium module. The mole fractions of NO and OH are about 0.051 and 0.0038 at the centerline of the plasma torch. The mole fractions of NO and OH were digitized from Fig. 3 in Ref. 8. The temperature of 3400 K was determined under the condition of local thermodynamic equilibrium.

Figure 5 shows the comparison between the measured spectrum and the computed spectrum with the effect of water vapor absorption at the temperature of 3400 K. The calculated spectra show the fundamental bands of NO at 5  $\mu\text{m}$ , and the lines of OH fundamental and of the NO first overtone between 2.5  $\mu\text{m}$  and 4.15  $\mu\text{m}$ . It is shown that the computed spectrum is underestimated compared to the measured spectrum between 4.2  $\mu\text{m}$  and 4.9  $\mu\text{m}$ . This is because the effect of carbon dioxide is absent in the present study. From Fig. 1, it can be deduced that the radiation spectrum is attenuated due to the contribution of the water

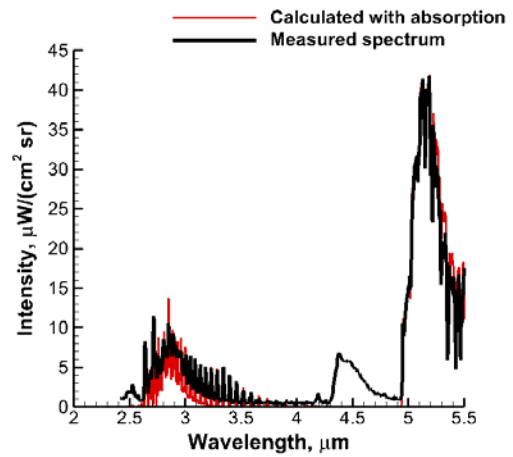


Fig. 5. Comparison between Measured Spectrum and Calculated Spectrum with Absorption over Range 2.5-5.5  $\mu\text{m}$ .

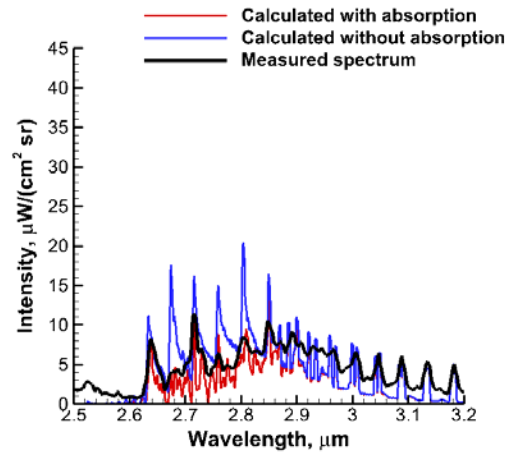


Fig. 6. Calculated Spectra with and without Absorption over Range 2.5-3.2  $\mu\text{m}$ , Compared to Measured Spectrum.

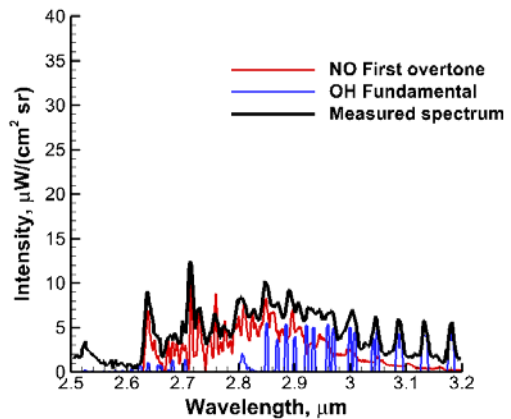


Fig. 7. Contributions of NO and OH Molecules with Absorption over the Range 2.5-3.2  $\mu\text{m}$ .

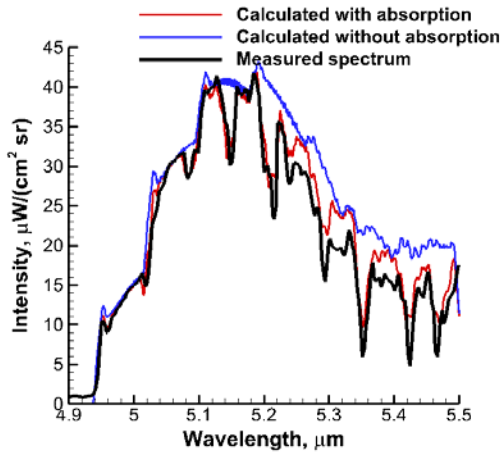


Fig. 8. Calculated Spectra with and without Absorption over Range 4.9-5.5  $\mu\text{m}$  Compared to Measured Spectrum.

absorption, especially in the range of 2.4-3.2  $\mu\text{m}$  and 4.9-5.5  $\mu\text{m}$ .

To distinguish the effect of water vapor absorption on the emission spectra more precisely, the synthetic spectra were focused in the range of 2.4-3.2  $\mu\text{m}$  and 4.9-5.5  $\mu\text{m}$ , as shown in Figs. 6-8. It is observed that the prediction with the absorption is in good agreement with the measured spectrum.

Figure 6 shows the simulated spectra with and without absorption, and the results are compared with the measured spectrum. While the calculated spectrum without absorption is overestimated and shows discrepancy in the absolute intensity, the calculated spectrum with water absorption is in good agreement and matches well with the measured spectrum.

The contribution of *NO* and *OH* molecules with water vapor absorption in the range of 2.4-3.2  $\mu\text{m}$  is presented in Fig. 7. It is shown that weak *R* branches of *OH* are located at around 2.5  $\mu\text{m}$ , and *P* branches of *OH* and the first overtone transition of *NO* are present 2.7  $\mu\text{m}$ .

Comparison was also made between the measurement and the computed spectra for *NO* fundamental bands in Fig. 8. It is observed that the fundamental transition of *NO* is positioned at 5  $\mu\text{m}$ . The rotational quantum number is extended to 90.5 to capture the band head of the fundamental rovibrational transition, since the given rotational quantum numbers are up to 59.5 in the Hamiltonian matrix for *NO* molecule.

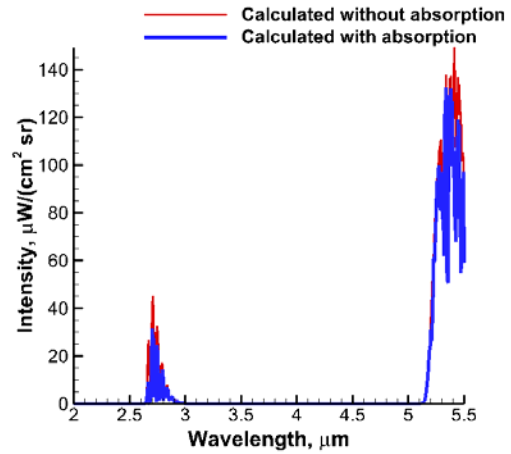


Fig. 9. Calculated Spectrum in Convergent-Divergent Nozzle with Effect of Absorption Under Thermal Nonequilibrium Condition.

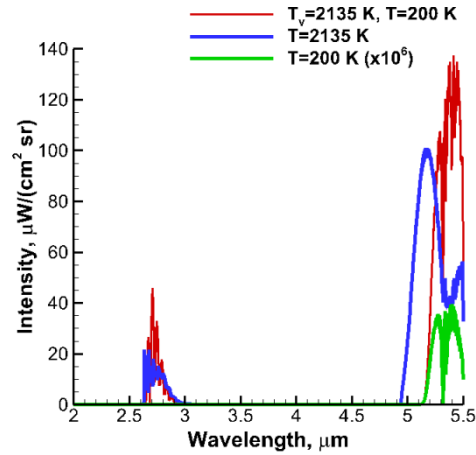


Fig. 10. Simulated Spectrum in Convergent-Divergent Nozzle under both Thermal Nonequilibrium Condition and Thermal Equilibrium Condition.

Thus, the band heads of (1-0) and (2-1) transitions are located at 4.95 and 5.03  $\mu\text{m}$ , respectively.

### 3.2 Thermal Nonequilibrium on Convergent-Divergent Nozzle

Next, estimation of the radiation intensity for *NO* molecule in a convergent-divergent nozzle under the thermal nonequilibrium condition was made. To calculate the spectrum under the thermal nonequilibrium, various temperature and mole fraction need to be determined. As mentioned above, the vibrational and translational temperatures obtained from Fig. 3 are 2135 K and 200 K, since other temperatures

were determined by using a two-temperature model. The mole fraction of  $NO$  is 0.0854.

Figure 9 shows prediction of the radiation intensity in the convergent-divergent nozzle under the thermal nonequilibrium condition. The results are also compared with those both with and without absorption in the range of 2.5-5.5  $\mu m$ . As shown in the figure, the radiating system of  $NO$  is clearly presented in the range of 2.5-3  $\mu m$  and 5-5.5  $\mu m$ , which corresponds to the first overtone and the fundamental rovibrational transition. In addition, the intensity is attenuated over the entire range due to the absorption.

For the comparison with those under the thermal equilibrium condition, simulations were made at temperatures of 2135 K and 200 K in Fig. 10. The simulated spectrum at the temperature of 200 K is multiplied by 10 to the power of six for comparison.

The results are also compared with those under the thermal nonequilibrium without the effect of absorption. It is shown that the  $NO$  fundamental transition under nonequilibrium occurs at about 5.1  $\mu m$  since the  $NO$  fundamental transition is located near 4.94  $\mu m$  at the local thermodynamic temperature of 2135 K. The thermal nonequilibrium simulation shows that highly intense emission in the range of 5.3-5.5  $\mu m$ , which shows a similar pattern with the result at 200 K. In the range of 2.5-3.2  $\mu m$ , the simulation under nonequilibrium shows peak points, which correspond to the first overtone transition of  $NO$ , as well as the calculated result at the temperature of 2135 K. The equilibrium simulation at 200 K does not occur in this region because of lower temperature.

#### 4 Conclusions

An infrared radiation modeling for  $NO$  and  $OH$  diatomic molecules was made for nonequilibrium radiation simulations. To validate the numerical radiation model, the calculated spectrum at a temperature of 3400 K was compared with the measured spectrum in the range of 2.5-5.5  $\mu m$ . It was shown that the simulated spectral intensity is in good

agreement with the measured spectrum. It was observed that weak  $R$  branches of  $OH$  are present at around 2.5  $\mu m$ , and  $P$  branches of  $OH$  and the fundamental and the first overtone transition of  $NO$  are located near 5  $\mu m$  and 2.7  $\mu m$ , respectively. In addition, assessment of room air absorption was performed by comparing the radiation intensity results without the effect of room air absorption. The radiation spectrum is attenuated by the absorption in the ranges of 2.4-3.2  $\mu m$  and 4.9-5.5  $\mu m$ .

The radiation intensity of the one-dimensional steady flow in a convergent-divergent nozzle under thermal nonequilibrium condition was also analyzed. It was observed that highly intense emission in the range of 5.3-5.5  $\mu m$  exists, and the pattern is similar to the results at same translational and rotational temperatures of 200 K.

#### Acknowledgement

This work was supported by the Low Observable Technology Research Center program of Defense Acquisition Program Administration and Agency for Defense Development.

#### References

- [1] D.R. Smith and M. Ahmadjian. Observation of nitric oxide rovibrational band head emissions in the quiescent airglow during the CIRRIS-1A space shuttle. *Geophysical Research letter*, Vol. 20, No. 23, pp. 2679-2682, 1993.
- [2] P.S. Armstrong, S.J. Lipson, J.A. Dodd, J.R. Lowell, W.A.M. Blumberg, and R.M. Nadile. Highly rotationally excited  $NO(v,J)$  in the thermosphere from CIRRIS 1A limb radiance measurements. *Geophysical Research letter*, Vol. 21, No. 22, pp. 2425-2428, 1994.
- [3] D.S. Babikian, N.K.J.M. Gopaul, and C. Park. Measurement and analysis of nitric oxide radiation in an arcjet flow. *Journal of Thermophysics and Heat Transfer*, Vol. 8, No. 4, pp. 737-743, 1994.
- [4] C. Schulz, V. Sick, J. Heinze, and W. Stricker. Laser-induced-fluorescence detection of nitric oxide in high-pressure flames with A-X (0,2) excitation. *Applied Optics*. Vol. 36, No. 15, pp. 3227-3232, 1997.

- [5] D.A. Levin, C.O. Laux, and C.H. Kruger. A general model for the spectral radiation calculation of OH in the Ultraviolet. *JQSRT*, Vol. 61, pp. 377-392, 1998.
- [6] I.D. Boyd, W.D. Phillips, and D.A. Levin. Sensitivity studies for prediction of ultraviolet radiation in nonequilibrium hypersonic bow-shock waves. *Proc. 35th Aerospace Sciences Meeting & Exhibit*, AIAA-97-0131, 1997.
- [7] C.O. Laux, R.J. Gessman, B. Hillber, and C.H. Kruger. Experimental study and modeling of infrared air plasma radiation. *Proc. 30th AIAA Thermophysics Conference*, AIAA 95-2124, 1995.
- [8] D.M. Packan, R.J. Gessman, L. Pierrot, C.O. Laux, and C.H. Kruger. Measurement and modeling of OH, NO, and CO<sub>2</sub> infrared radiation in a low temperature air plasma. *Proc. 30th AIAA Plasmadynamics and Lasers Conference*, AIAA-1999-3605, 1999.
- [9] C. Park. *Nonequilibrium hypersonic aerothermodynamics*. John Wiley & Sons, Inc., 1990.
- [10] S.-Y. Hyun. *Radiation code SPRADIAN07 and its application*. Ph.D Thesis, 2009.
- [11] C. Amiot. The infrared emission spectrum of NO: Analysis of the  $\Delta v = 3$  sequence up to  $v=22$ . *Journal of Molecular Spectroscopy*, Vol. 94, No. 1, pp.150-172, 1982.
- [12] G. Stark, J.W. Brault, and M.C. Abrams. Fourier-transform spectra of the  $A^2\Sigma^+ - X^2\Pi$   $\Delta v = 0$  bands of OH and OD. *J. Opt. Soc. Am. B.*, Vol. 11, No. 1, pp. 3-32, 1994
- [13] J.R. Gillis and A. Goldman. Nitric oxide IR line parameters for the upper atmosphere. *Applied Optics*, Vol. 21, No. 7, pp. 1161-1163, 1982.
- [14] S.R. Langhoff and C.W. Jr Bauschlicher. Theoretical dipole moment for the  $X^2\Pi$  state of NO. *Chem. Phys. Letter*, Vol. 223, pp. 416-422, 1994. Vol. 49, No. 3, pp. 223-235, 1993.
- [15] K.W. Holtzclaw, J.C. Person and B.D. Green. Einstein coefficients for emission from high rotational states of the OH ( $X^2\Pi$ ) radical. *JQSRT*, Vol. 49, No. 3, pp. 223-235, 1992.
- [16] L.S. Rothman, I.E. Gordon, R.J. Barber, H. Dothe, R.R. Gamache, A. Goldman, V.I. Perevalov, S.A. Tashkun, J. Tennyson. HITEMP, the high-temperature molecular spectroscopic database. *JQSRT*, Vol. 111, pp. 2139-2150, 2010.
- [17] L.S. Rothman, D. Jacquemart, A. Barbe, C. Chris Benner, M. Birk, L.R. Brown, M.R. Carleer, C. Chackerian Jr., K. Chance, L.H. Coudert, V. Dana, V.M. Devi, J.-M. Flaud, R.R. Gamache, A. Goldman, J.-M. Hartmann, K.W. Jucks, A.G. Maki, J.-Y. Mandin, S.T. Massie, J. Orphal, A. Perrin, C.P. Rinsland, M.A.H. Smith, J. Tennyson, R.N. Tolchenov, R.A. Toth, J. Vander Auwera, P. Varanasi, and G. Wagner. The HITRAN 2004 molecular spectroscopic database. *JQSRT*, Vol. 96, pp. 139-204, 2005.
- [18] C. Park and S.H. Lee. Validation of multitemperature nozzle flow code. *Journal of Thermophysics and Heat Transfer*, Vol. 9, No. 1, pp. 9-16, 1995.
- [19] W.N. MacDermott and J.G. Marshall. Nonequilibrium nozzle expansions of partially dissociated air: a comparison of theory and electron-beam experiments. AEDC-TR-69-66, 1969.

### Copyright Statement

The authors confirm that they, and/or their company or organization, hold copyright on all of the original material included in this paper. The authors also confirm that they have obtained permission, from the copyright holder of any third party material included in this paper, to publish it as part of their paper. The authors confirm that they give permission, or have obtained permission from the copyright holder of this paper, for the publication and distribution of this paper as part of the ICAS2012 proceedings or as individual off-prints from the proceedings.